

## Texture and Mechanical Properties of Al-Mg-Si Series Aluminum Alloy Sheets Manufactured by Cross-roll Rolling Method

Kwang-Jin Lee<sup>1</sup>, Jae-Yeol Jeon<sup>1</sup>, Hyeon-Taek Son<sup>1</sup> and Kee-Do Woo<sup>2</sup>

<sup>1</sup>Automotive Components Center, Korea Institute of Industrial Technology,  
1110-9 Oryung-dong, Buk-gu, Gwangju, 500-480, Korea

<sup>2</sup>Division of Advanced Materials Engineering & Research Center of Industrial Technology,  
Chonbuk National University, Chonbuk 561-756, Korea

Relationship between texture and mechanical properties of 6xxx aluminum alloy sheets processed by cross-roll rolling was investigated. Microstructures of normal-roll rolled and cross-roll rolled sheets after solution heat treatment (SHT) were analyzed by optical micrographs (OM). Texture distribution through thickness in 6xxx aluminum alloy normal-roll and cross-roll rolled sheets after SHT has been investigated using the electron back-scattered diffraction (EBSD) technique. Analyses of texture in three layers from the surface to the center of the sheet were performed. The texture of normal-roll rolled sheet after SHT consists of recrystallization textures: cube{001}<100> and rotated cube. However, the texture of cross-roll rolled sheet after SHT is composed of random and weak  $\beta$ -fiber texture. R-value of cross-roll rolled sheet is about 30% higher than normal-roll rolled sheet. From the result of limit dome height test (LDH) cross-roll rolling is effective to improve the formability of 6xxx aluminum alloy.

**Keywords:** Cross-roll rolling, Texture, shear deformation, R-value, Limit dome height test.

### 1. Introduction

The use of Al alloys is expanding, particularly in the automobile industry. Even though the high strength of aluminum alloy containing Mg and Si (6xxx series aluminum alloy) can be easily achieved, the formability of aluminum alloy is insufficient to meet the demands. Hence, many researchers are attracted to the study and development on the improvement of formability by means of heat treatment, precipitation and rolling technology. It is well known that texture may be inhomogeneous through the thickness of rolled sheets due to the inhomogeneity of the deformation during rolling [1-4] and the non-uniformity of the recrystallization that occurs during the heat treatment [5]. And the crystallographic texture significantly influences the mechanical properties of the aluminum alloy sheets. In order to improve formability of aluminum alloy, instead of normal-roll rolling, cross-roll mill was used during cold rolling in this study. Cross-roll rolling is a new rolling method proposed by Chino and in this new rolling method, the roll axis is tilted against transverse direction (TD) in rolling direction (RD)-TD plane as shown in Fig. 1. Chino et al. reported that cross-roll rolling was effective in that thrust force in an axial direction of a roll can be imposed on a rolled sheet, and intense shear deformation in normal direction (ND) can be easily imposed on a sheet, leading to a refinement of the microstructure and an improvement in formability of magnesium alloy sheets [6]. The aim of this study is to understand the texture distribution through thickness in 6xxx aluminum alloy sheet fabricated by cross-roll rolling and how much texture control affects strength, anisotropy and formability of 6xxx aluminum alloy sheet by cross-roll rolling method.

Table 1 Chemical compositions of the alloy [mass%].

| Alloy  | Mg  | Si  | Cu  | Mn  | Others | Al   |
|--------|-----|-----|-----|-----|--------|------|
| AA6xxx | 0.5 | 1.0 | 0.5 | 0.1 | 0.1    | Bal. |

## 2. Experiment

The material used in the present study was 6xxx aluminum alloy which was modified alloy between AA6016 and AA6111. The chemical composition of this alloy is given in Table 1. A pre-heated 6xxx aluminum alloy plate of 10mm in thickness was rolled to 2.5mm by about 75% reduction under lubricant during hot rolling and subsequently annealed at 400°C for 1hr. The annealed hot strip was cold rolled by four passes of cross-roll rolling and normal rolling with maintaining the original RD to a thickness of 1.0mm, corresponding to a thickness reduction of 60%. Cross-roll rolling was carried out in a laboratory rolling mill in which the roll axes are tilted by  $\pm 5^\circ$  away from the TD in the RD-TD plane (Fig. 1). In the present study, so as to increase shear deformation cross-roll rolling was conducted without lubricant. More details on the method of cross-roll rolling can be found in Refs. [6]. The 1.0mm thick sheet was fully solutionized at 500°C for 1hr. The 1.0mm thick sheet was mechanically polished and then electro-polished in a solution consisting of 70% ethanol, 12% distilled water, 7.8% perchloric acid and 10% butoxyethanol to remove the deformation layer. The electron back-scatter diffraction (EBSD) analysis was conducted on the ND surface of the sheet extending from the surface to the mid-thickness. The observed position was described by the parameter S which was defined by the equation:

$$S = \Delta t / t_0 \quad (1)$$

where  $\Delta t$  is the distance from the center, and  $t_0$  the sheet thickness. Three typical zones were selected from the center to the subsurface through the plate thickness, with 0, 0.47 and 0.95 respectively. R-values were determined in tensile tests. And the press formability of cross-roll rolled sheets was compared with that of unidirectional rolled sheets determined by limit dome height test (LDH) at room temperature.

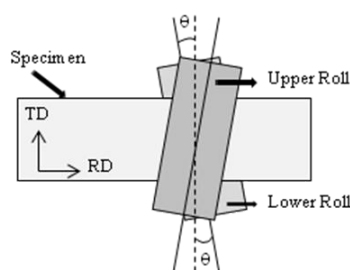


Fig. 1 The schematic view of cross-roll rolling.

## 3. Results and Discussion

### 3.1 Recrystallized microstructure

As mentioned above, Chino et al. reported that cross-roll rolling led to a refinement of the microstructure and an improvement in formability of magnesium alloy sheets [6]. In order to investigate the effect of cross-roll rolling on the evolution of microstructure after recrystallization in 6xxx aluminum alloy, sheets taken from the two kinds of differently rolled (normal-roll rolled and cross-roll rolled) sheets were fully solutionized at 500°C for 1hr. The resulting microstructures were analyzed by optical micrographs and grain size of three layers (surface, quarter and middle) was measured by EBSD (EBSD maps which are surrounded by grain boundaries with misorientations exceeding  $15^\circ$  from their neighborhood). Fig. 2 shows the distribution of grains in the two recrystallized sheets, where the sheet surface and bottom are specified. The grain sizes achieved at the various through-thickness layers in both samples are listed in Table 2. The normal-roll rolled sample shows a rather inhomogeneous recrystallized grain size through the thickness

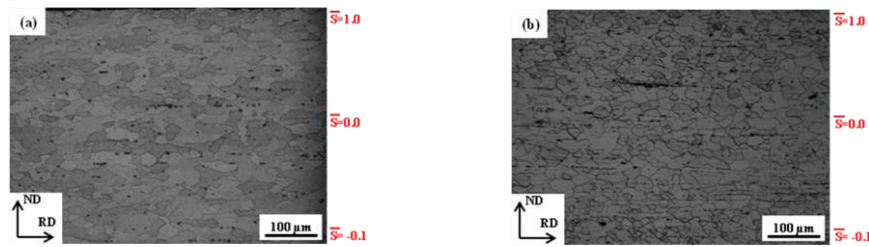


Fig. 2 Optical micrographs on the TD-plane of normal-roll cold rolled (a) and cross-roll cold rolled (b) sheets after SHT.

with an average grain size of  $58\mu\text{m}$  near the surface and grains larger than  $65\mu\text{m}$  in the quarter and center layers. This decrease in grain size reflects the increase of shear strain near the surface caused by appreciable amounts of shear deformation  $\dot{\epsilon}_{13}$  generated because of the geometrical shape change in a roll gap and the friction between the sample surface and rolls[7,8]. The cross-roll rolled sheet shows a finer, more uniform recrystallized microstructure in all layers, which decreases slightly with increasing  $s$ .

Table 2 Recrystallized grain size (in  $\mu\text{m}$ ) derived from the EBSD grain boundary maps.

|                     | S=0.0 | S=0.47 | S=0.95 |
|---------------------|-------|--------|--------|
| Normal-roll rolling | 75    | 65     | 58     |
| Cross-roll rolling  | 49    | 42     | 38     |

This is because the characteristic of cross-roll rolling geometry imposes shear strains ( $\dot{\epsilon}_{12}$ ,  $\dot{\epsilon}_{13}$  and  $\dot{\epsilon}_{23}$ ) on the whole sheet [9] (where the rolling direction (RD), transverse direction (TD) and normal direction (ND) of a sheet are identified by direction 1, 2 and 3 respectively). Especially, the finer grain size throughout the cross-roll rolled sheet compared to normal-roll rolled sheet may be attributed to the high, uniform shear strain  $\dot{\epsilon}_{23}$ . This means that cross-roll rolling leads to a refinement of the microstructure of 6xxx aluminum alloy after recrystallization.

### 3.2 ODF analysis

The Orientation Distribution Function (ODF) measured from the normal-roll and cross-roll rolled samples after solution heat treatment (SHT) displayed a pronounced deviation from the orthotropic sample symmetry; therefore, the ODF was calculated in the Euler angle range of  $\{0^0 \leq \varphi_1, \Phi, \varphi_2 \leq 90^0\}$ [10,11]. Fig. 3 shows the ODF of normal-roll cold rolled sheet after SHT at  $500^\circ\text{C}$  for 1hr for analysing recrystallization texture. The recrystallization texture of normal-roll cold rolled sheet after SHT shows the formation of typical recrystallization texture; cube $\{001\}\langle 100\rangle$  of fcc material having high stacking fault energy in Fig. 3(a). In details near the surface ( $s=0.95$ ) the well-known cube recrystallization texture developed which were characterized by preferred orientations with maximum texture intensities of  $f(g)_{\text{max}}=16.2$  and rotated cube $\{001\}\langle 130\rangle$  and  $\{001\}\langle 110\rangle$  and also found with other weak shear textures caused by shear component  $\dot{\epsilon}_{13}$  in  $\varphi_2 = 0^0$  section. And Cube and rotated cube are preferred orientation but weak Cu $\{112\}\langle 111\rangle$  and Bs $\{011\}\langle 211\rangle$  orientations exist in  $\varphi_2 = 45^0$  section. The quarter layer( $S=0.47$ ) seems to serve as a transition layer between surface and middle layers in which cube $\{001\}\langle 100\rangle$  with maximum intensities of  $f(g)_{\text{max}}=17.4$  and Bs $\{011\}\langle 211\rangle$  are dominating in  $\varphi_2 = 0^0$  section in Fig. 3(b). Fig. 4 shows the ODF of cross-roll cold rolled sheet after SHT at  $500^\circ\text{C}$  for 1hr for analysing recrystallization texture. the texture near the surface of the cross-roll rolled samples comprise the  $\beta$ -fiber-like o

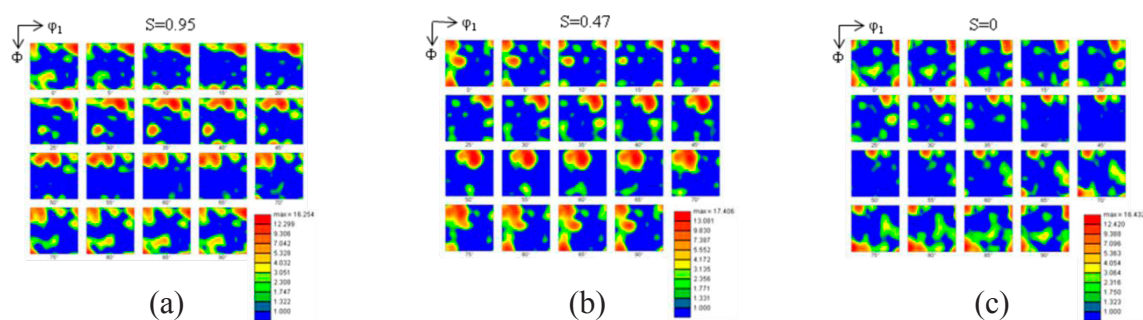


Fig. 3 Texture of normal-roll cold rolled sheet after SHT at (a) surface layer( $s=0.95$ ), (b) middle layer( $s=0.47$ ) and (c) center layer( $s=0.0$ ).

orientations (Cu, S and Bs), which runs through orientation space from the Cu  $\{112\}\langle 111\rangle$  orientation over the S  $\{123\}\langle 634\rangle$  orientation to  $\{012\}\langle 142\rangle$  random texture. Furthermore, a scatter of  $\{001\}\langle 110\rangle$  orientation toward  $\{112\}\langle 110\rangle$  orientation and  $\{111\}\langle 110\rangle$  orientation are also found. The resulting ODF is weak with a texture maximum  $f(g)_{\max}=6.7$  compared to the ODF of normal-roll rolled sheet after SHT in Fig. 4(a). The quarter layer( $S=0.47$ ), however, seems to serve as a transition layer, in which the  $\beta$ -fiber with a scattering of shear texture and random

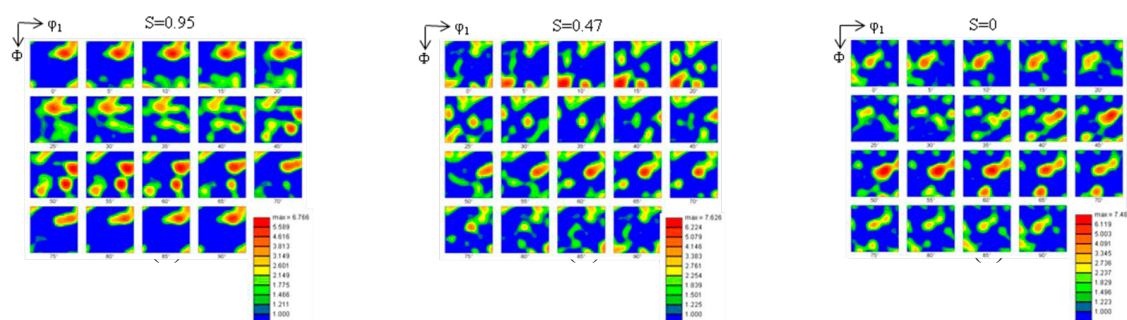


Fig. 4 Texture of cross-roll cold rolled sheet after SHT at (a) surface layer( $s=0.95$ ), (b) middle layer( $s=0.47$ ) and (c) center layer( $s=0.0$ ). textures by cross-roll rolling appeared. The texture in the center layer of the sheet comprises Bs, S and weak Cu with shear texture;  $\{011\}\langle 100\rangle$ ,  $\{021\}\langle 100\rangle$  and very weak cube and rotated cube were found. Generally the rolling texture of normal cold-rolled sheet was composed of a  $\beta$ -fiber in aluminum alloy and after recrystallization  $\beta$ -fiber especially, Cu and S changed to Cube orientation. However, a greater modification of the normal-roll rolling texture by means of the cross-roll rolling gives rise to a greater deviation from the conventional recrystallization texture and it is proven by the ODF results that all layers of cross-roll rolled sheet after SHT show randomized texture and weak  $\beta$ -fiber texture. Operation of shear components along TD - i.e.  $\dot{\epsilon}_{12}$ ,  $\dot{\epsilon}_{13}$  and  $\dot{\epsilon}_{23}$  is expected during cross-roll rolling. Even though recrystallization textures of cube and rotated cube orientation after SHT were shown in all layers, a weak  $\beta$ -fiber and random textures were dominating. Because a large uniform shear strain  $\dot{\epsilon}_{23}$  is imposed in the whole sheet thickness by means of cross-roll rolling [9].

### 3.3 Formability

With regard to the aim of improving the formability of 6xxx aluminum alloy sheet by cross-roll rolling, the Lankford parameters (R-value) of the differently processed sheets were analyzed. R-values were determined in tensile tests from the ratio between the in-plane and the through-

thickness strain for angles of  $\alpha = 0, 45$  and  $90^\circ$  between tensile direction and rolling direction. For each value, three specimens were analyzed. Fig. 5 shows the results for both the normal-roll rolled -

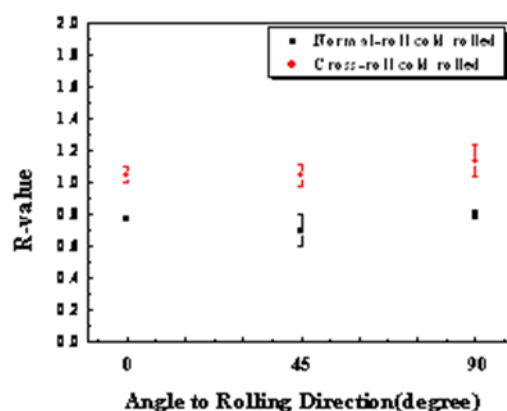


Fig. 5 Variation of R-values of the solution heat treated specimens of normal-roll rolled and cross-roll rolled sheets.

sheet and the cross-roll rolled sheet after SHT. Furthermore, an average value,  $\bar{R}$ , was determined:

$$\bar{R} = \frac{R_{0^\circ} + 2R_{45^\circ} + R_{90^\circ}}{4} \quad (2)$$

where the subscripts 0, 45, 90<sup>0</sup> indicate the tensile direction. The normal-roll rolled sheet yielded R-values of 0.76 in the RD, 0.8 in the TD and a minimum of  $R=0.7$  at  $\alpha=45^\circ$ ; the average value,  $\bar{R}$ , is about 0.74. This rather unfavorable behavior of  $R(\alpha)$  is typical of aluminum alloy sheets with a cube recrystallization texture [12]. For the cross-roll rolled sheet the individual  $R(\alpha)$ -values were notably higher, between 1.0 and 1.1 in the RD and the TD and 1.0 for  $\alpha=45^\circ$ . This results in an average R-value of as much as  $\bar{R}=1.0$ .

### 3.4 Limit dome height test (LDH)

Limit dome height tests were conducted at room temperature and the tool geometric parameters

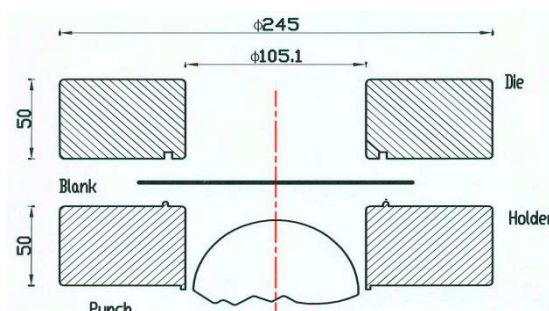


Fig. 6 Tool geometry of LDH test

are given in Fig. 6. The sheets after LDH test are shown in Fig. 7, where (a) the size of specimen is 195x110x1(mm) and (b) 195x120x1(mm). The LDH value was measured to be 29.5mm for normal-roll rolled sheet and 31.5 mm for cross-roll rolled sheet after SHT in Fig. 7(a) and 27.5mm for normal-roll rolled sheet and 30.0mm for cross-roll rolled sheet after SHT in Fig. 7(b). Thus, press formability of the cross-roll rolled sheet was higher than that of the normal-roll rolled sheet at all testing sheets.

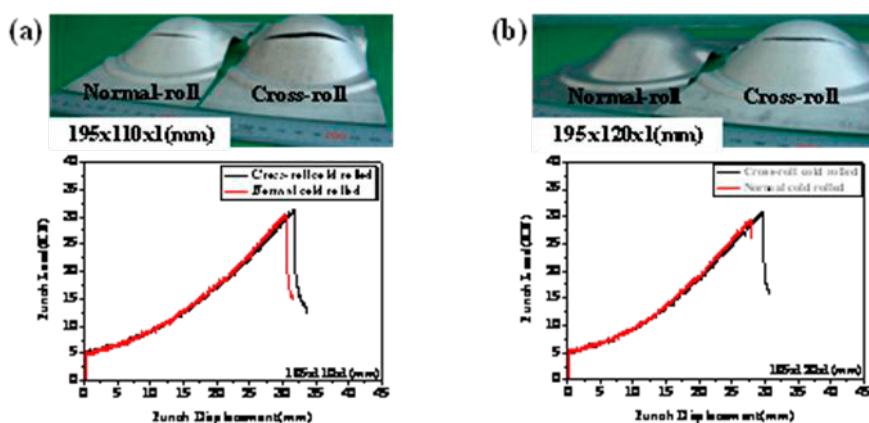


Fig. 7 The specimens after LDH tests and punch load versus punch displacement curves at different blank diameters (a)195x110x1(mm) and (b)195x120x1(mm).

#### 4. Conclusion

We have studied the texture distribution in 6xxx aluminum alloy sheet fabricated by cross-roll rolling method during cross-roll rolling in which the roll axes tilted by  $\pm 5^{\circ}$  away from the transverse direction of the rolled sample. Cross-roll rolling leads to a refinement of the microstructure of 6xxx aluminum alloy after SHT compared to normal-roll rolling and the cross-roll rolled sheets depicted textures with very weak  $\{001\}\langle 100\rangle$  cube intensities. Randomized texture and  $\beta$ -fiber texture could be achieved on the whole sheet by the characteristic of cross-roll rolling geometry that imposes shear strains ( $\dot{\epsilon}_{13}$ ,  $\dot{\epsilon}_{12}$  and  $\dot{\epsilon}_{23}$ ). With regard to the formability of the resulting sheets, the cross-roll rolled sheets exhibited significantly higher R-values than the normal-roll rolled sheets. The resulting homogeneous planar anisotropy with high  $R(\alpha)$  values leads to improved formability of the cross-roll rolled sheets and relates to press formability.

#### References

- [1] O. V. Mishin, B. Bay, D. Juul Jensen: Metall. Mater. Trans. A 31 (2000) 1653-1662.
- [2] O. Engler, M.Y. Huh, C.N. Tomé: Mater. Trans. A 31 (2000) 2299-2315.
- [3] W.C.Liu, J.G. Morris: Mater. Trans. A 36 (2005) 1329-1338.
- [4] H. Jazaeri, F.J. Humphreys: Acta Mater. Vol. 52 (2004) 3251-3262.
- [5] M.P. Miller, T.J. Turner: Int. J. Plast. 17 (2001) 783-805.
- [6] Y. Chino, K. Sassa, A. Kamiya, M. Mabuchi: Mater. Sci. Eng. A 441 (2006) 349-356.
- [7] J.J. Nah, H.G. Kang, M.Y. Huh, and O. Engler, Scripta Mater. 58 (2008) 500-503.
- [8] H.G. Kang, J.K. Kim, M.Y. Huh, and O. Engler, Mater. Sci. Eng. A 452-453 (2007) 347-358.
- [9] S.H. Kim, H.G. Kang, M.Y. Huh, O. Engler: Mater. Sci. Eng. A 508 (2009) 121-128.
- [10] H.J. Bunge, Texture Analysis in Materials Science, Butterworths, London (1982).
- [11] V. Randle, O. Engler, Introduction to Texture Analysis: Macrotexture, Microtexture and Orientation Mapping, Gordon and Breach Sci. Publ., Amsterdam (2000).
- [12] O. Engler, J. Hirsh, Mater. Sci. Forum 479 (1996) 217-222.